# INFLUENCE OF SOME STRUCTURAL PARAMETERS ON BOTH THEORETICAL AND EXPERIMENTAL COMPRESSIVE STRENGTH OF LAMINATES

S. Drapier [1], L. Daridon [2], and J.-C. Grandidier [3]

[1] Now at : *Mechanical and Materials Eng. Dept., Ecole Nat. Sup. des Mines de Saint-Etienne 158 Cours Fauriel, 42023 Saint-Etienne cedex02, France*
[2] *Laboratory for the Mechanics of Industrial Multi-Material Université Louis Pasteur, rue du maréchal Lefèbvre, 67100 Strasbourg, France*
[3] Now at : *Laboratory of Mechanical Modelling and Applied Mathematics SP2MI, Boulevard 3, Téléport 2, BP179, 86960 Futuroscope cedex, France*

**SUMMARY :** It is now well established that the axial compressive strength of long-fibre composites is limited by the development of a local mechanism called microbuckling which depends strongly on the coupling of fibre initial geometric imperfection with the resin non-linear shear behaviour. Besides this local phenomenon, failure strains measured experimentally depend also on some structural parameters at the ply scale, effect of which is less well known. We have been investigating for several years the effect of these structural parameters, called *structure effect*, from both an experimental and a theoretical point of view. A model that is able to account for both local and structural parameters, with reasonable computation amounts, was proposed recently. Meanwhile, thanks to a thoroughfull examination of some existing experimental devices, new designs were proposed for both compression and bending-compression tests. Here, by cross-checking the results of these complementary studies is demonstrated the necessity of accounting for the structure effect to design composite structures against compression.

**KEYWORDS**: compressive strength, plastic microbuckling, structure effect, mesoscopic modelling, geometric imperfection, experimental device.

## INTRODUCTION

Predicting the mechanical behaviour of organic long fibre composites is in essence a difficult task. While recent research allows a better grasp of the main problems, the situation is still not clear as far as the compressive behaviour in fibre direction is concerned. Although this problem has been extensively studied for more than 30 years, predictions can sparsely correlate experimental results. Moreover, improvements brought to fibre strength are not passed on the measured laminate compressive characteristics.

Measurement of the compressive strength is usually achieved with pure compression devices which are hardly reliable in characterising the compressive strength as failure initiates in the grips wherein 3-dimensional stress state develop. In GARTEUR program [1] scatters of up to 47% are observed between experimental strengths of the same material measured by several laboratories. Stress failure measurements seem to be more representative of the experimental procedure than of the material itself. Experimental work reported in the literature shows that (i) ultimate failure stress under compression is lower than under tension and that (ii) in

laminates the larger the number of consecutive plies in the loading direction, the lower their strength [2] [3].

This scatter of results from pure compression tests can be largely reduced by using bending-compression test fixtures. The loading induced in the specimen is in that case more homogeneous and failure generally takes place on the compressed face in the centre of the specimen. With such devices, the influence of the structure at mesoscopic scale on the compressive failure of UD plies has been clearly established : Ref. 4 showed that thickening the specimen lowers the strength, Ref. 5 established that a high gradient of loading across the specimen thickness increases the compressive strength. Ref. 6 and Ref. 7 recently confirmed these results, using a pin-ended buckling device wherein hinge rotations can be restrained.

This suggests that (i) the use of pure compression devices lead to a very poor estimation of the actual strength and that (ii) the difference in strength reached under the two types of loading is related to the ability to generate pure stress states. Moreover, regardless the scatter of pure compression test results, this also suggests an effect of the failure mechanism upon the large difference between measurements made under bending and compression loading. If early research traced the origin of failure to the development of local plastic microbuckling [8] [9] the effect of the structure at ply scale (and hence the effect of the type of loading) on the failure mechanism of laminated composites has been studied only recently [5] [10]. Since then, we have been extensively investigating such *structure effect* from both an experimental [5] [7] [10] and a theoretical point of view [10] [11] [12]. Here we aim at cross-checking predictions from a model of plastic microbuckling including structure effect and experimental results obtained with in-different experimental test fixtures.

## MODELLING APPROACH

It is now well understood that microbuckling leads to the development of kink-bands which result in failure. Basically, two approaches can be distinguished : the kink-band modelling ([8] [9] for instance) and the study of the plastic microbuckling stability ([13] for instance). Yet the structure effect is very seldom taken into account, while experimentally its importance has been demonstrated several times. In order to account for the influence of the structure on the microscopic instability, a non-linear microbuckling model is set at mesoscopic scale, aimed at describing the failure mechanism with low computation load but accounting for every influent parameter [12]: size and shape of the fibre initial geometric imperfection, drop of stiffness induced by the plastic response of the matrix, and structural data across the laminate thickness.

### Formulation

A bidimensional representation of a laminate is used (Fig. 1) where $\mathbf{e_1}$ is the 0° direction corresponding to the loading direction. Displacement along $\mathbf{e_1}$ is u and displacement along $\mathbf{e_2}$ is v. Stresses (second Piola-Kirchhoff tensor) are denoted $\mathbf{S}$ and Green-Lagrange's strain tensor is $\boldsymbol{\gamma}$. Based on works of Ref. 5 and Ref. 10, a formulation of the plastic microbuckling problem can be proposed where the virtual powers equation (Eqn 1) and the constitutive law (Eqn 2) write :

$$-\int_{\Omega} \{f\, E_f\, r_{gf}^2\, v''\, \delta v'' + \mathbf{S}.\delta\boldsymbol{\gamma}\}\, d\Omega + \langle \mathbf{F}, \delta\mathbf{u} \rangle = 0, \forall\, \delta\mathbf{u} \qquad (1)$$

$$\mathbf{S}(\boldsymbol{\gamma}) = \mathbf{L}(\boldsymbol{\gamma}).\boldsymbol{\gamma} \qquad (2)$$

where f is the fibre volume fraction, $E_f$ is the fibre Young's modulus, $r_{gf}$ is the fibre gyration radius and where **F** represents the external loading. The constitutive law (Eqn 2) is of anisotropic type, the secant modulus tensor **L** being obtained from an explicit homogenisation formula based upon the constituents behaviour [14]. Plasticity is defined at microscopic scale to describe simply the anisotropy induced by fibre. Then only matrix material is non-linear and follows an isotropic law of $J_2$ deformation type that yields good predictions of plastic buckling [15].

This medium is not classical due to the first term of Eqn 1 which represents the fibre bending stiffness and that is essential in predicting the effect of the structural data [14] [11]. The presence of this bending term has been justified by a homogenisation study using the multi-scale method [14] and also by comparing modes and buckling loads from this approach with micro-heterogeneous modelling results [11].

Considering mainly uniaxial loading, non-linear terms in the strain tensor are reduced to terms in the loading direction. Initial fibre misalignment is represented with a 'deflection field' $v_0(\mathbf{x})$ defining the fibre initial position. Then the strain tensor writes (Eqn 3):

$$\boldsymbol{\gamma}(\mathbf{u}) = \boldsymbol{\varepsilon}(\mathbf{u}) + \gamma(\mathbf{u})_{11}^{NL}\, \mathbf{e}_1 \otimes \mathbf{e}_1$$

$$\text{with } \boldsymbol{\varepsilon}(\mathbf{u}) = \begin{pmatrix} \dfrac{\partial u}{\partial x_1} & \dfrac{1}{2}\left(\dfrac{\partial u}{\partial x_2} + \dfrac{\partial v}{\partial x_1}\right) \\ \dfrac{1}{2}\left(\dfrac{\partial u}{\partial x_2} + \dfrac{\partial v}{\partial x_1}\right) & \dfrac{\partial v}{\partial x_2} \end{pmatrix} \text{ and } \gamma(\mathbf{u})_{11}^{NL} = \frac{1}{2}\left(\frac{\partial v}{\partial x_1}\right)^2 + \frac{\partial v}{\partial x_1}\frac{\partial v_0}{\partial x_1} \tag{3}$$

**Mesoscopic approach**

Usually a numerical approach can be deduced from the continuous formulation through an adequate discretisation. In the present case, a further refinement is introduced which leads to a tractable model to represent at ply scale this local short-wavelength phenomenon. The solution of the microbuckling problem is sought under the form of a displacement field (Fig.1 and Eqn 4) evolving at the scale of the structure (denoted $\mathbf{u}_G$), very locally modulated by a displacement field evolving at the ply scale (denoted $\mathbf{u}_L$). With the hypothesis of quick variations of $\mathbf{u_L}$ and slow variations of $\mathbf{u_G}$, the strain tensor can be simplified (Eqn 5) .

$$\mathbf{u}(\mathbf{x}) = \mathbf{u}_G(\mathbf{x}) + \mathbf{u}_L(\mathbf{x}) \tag{4}$$

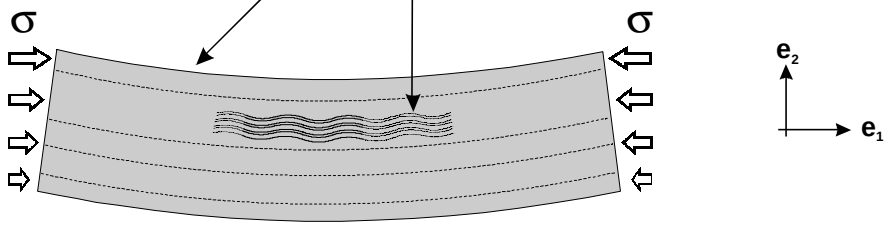


*Figure 1 : splitting of the displacement field.*

$$\boldsymbol{\gamma}(\mathbf{u}) = \boldsymbol{\gamma}_G(\mathbf{u}_G) + \boldsymbol{\gamma}_L(\mathbf{u}_L)$$

$$\text{with } \boldsymbol{\gamma}_G(\mathbf{u}_G) = \boldsymbol{\varepsilon}(\mathbf{u}_G) + \left(\frac{v_G'^2}{2}\right)\mathbf{e}_1 \otimes \mathbf{e}_1 \text{ and } \boldsymbol{\gamma}_L(\mathbf{u}_L) = \boldsymbol{\varepsilon}(\mathbf{u}_L) + \left(\frac{v_L'^2}{2} + v_L'\, v_0'\right)\mathbf{e}_1 \otimes \mathbf{e}_1 \tag{5}$$

With these approximations (Eqn 3 and Eqn 4) and assuming that displacement $\mathbf{u_G}$ is a known solution of equilibrium equations (Eqn 1 and Eqn2), one gets the variational equation describing the mesoscopic equilibrium, solution of which is $\mathbf{u_L}$ (Eqn 6) :

$$\int_{\Omega} \{ f\, E_f\, r_{gf}^2\, v_L''\, \delta v_L'' + \mathbf{S}_L(\boldsymbol{\gamma}_G,\boldsymbol{\gamma}_L).\delta\boldsymbol{\gamma}_L + S_{11}(\boldsymbol{\gamma}_G)\,(v_L'+v_0')\,\delta v_L' \} d\Omega = 0,\ \forall\ \delta\mathbf{u}_L \qquad (6)$$

where $\mathbf{S}_L(\boldsymbol{\gamma}_G,\boldsymbol{\gamma}_L) = \mathbf{S}(\boldsymbol{\gamma}_G+\boldsymbol{\gamma}_L)-\mathbf{S}(\boldsymbol{\gamma}_G)$. One may notice that in this mesoscopic formulation the external loading no longer appears and is replaced by the global field (Eqn 6). To simplify the problem, the global strain tensor is limited to its axial component (Eqn 7), corresponding to a global displacement induced by compression or bending-compression states :

$$\boldsymbol{\gamma}_G = \gamma_{G11}\, \mathbf{e}_1 \otimes \mathbf{e}_1 \qquad (7)$$

**Displacement approximation**

In the framework of cellular instabilities, the displacement field approximation is chosen as a product of amplitude across the ply thickness with few Ritz basis functions in the fibre direction. This hypothesis also allows reduction of the bidimensional domain studied to a single wavelength in the fibre direction, greatly reducing computations. Ritz basis functions are selected so that both microbuckling elastic modes obtained in Ref. 11 can be reproduced, and that a quasi-constant buckling stress can be obtained. Eventually, the displacement approximation is (Eqn 8) :

$$\mathbf{u}(\mathbf{x}) = \begin{cases} U_1(x_2)\cos(k\,x_1) + U_2(x_2)\sin(2k\,x_1) \\ \\ V_1(x_2)\sin(k\,x_1) + V_2(x_2)\sin(3k\,x_1) \end{cases} \qquad (8)$$

where k is the wavenumber and functions $U_i(x_2)$, $V_i(x_2)$ are the magnitudes of the displacement field which are discretised by three-noded finite element of Lagrange type. The imperfection is assumed to have a similar form, here we consider a combination of two sinusoids with a variable amplitude across the thickness and with wavelengths of k and 3k respectively (Eqn 9):

$$v_0(\mathbf{x}) = V_{01}(x_2)\sin(k\,x_1) + V_{02}(x_2)\sin(3k\,x_1) \qquad (9)$$

There is thus no limitation to any distribution across the laminate thickness, which is important in order to take account for the influence of structural parameters. Conversely, the Ritz approximation in the axial direction is more restrictive and this is what limits proper representation of the localisation of the instability. Consequently we focus on the response up to the maximum load corresponding to the instability occurrence.

## EXPERIMENTS

Study of the ‘Aérospatiale device’ (Fig. 3-a) is presented which leads to a rigorous explanation of the large scatter of measurements. We use finite element modelling with the commercial code ABAQUS to determine the stress state in the whole system. Except the glue that is assumed elasto-plastic, other materials are taken linearly elastic. Loading is prescribed so as to induce a 1% longitudinal strain in the gage section, corresponding to the experimental limit

An elastic singularity appears at the free tip of the tab [7] (abscissa 45 in Fig. 3-a). This over-stress leads quickly the glue in a plastic state which propagates in the whole tab towards the grip back and results in strains that exceed failure values. To take this into account an elasto-plastic law incorporating damage is developed based on video-driven shear tests carried out on an epoxy type glue by partners (Prof. C. G'sell and Critt Apollor at "Ecole des Mines de Nancy"). Introduction of plasticity coupled with damage lowers the global stress level in the specimen as well as the concentration at the tab tip. Computations also confirm massive failure of the glue, and then loading mode is no longer combined but tends towards an end specimen loading. This result perfectly fits with kink-band failure observed by Ref. 2.

We also investigate the effect of a positioning default due to imprecision in tooling the set-up, especially defect of parallelism between the plates applying the compressive load. Stress distribution in the specimen is shown in Fig. 2 for two defect amplitudes (0.05° et 0.5°). A large defect of 0.5° increases drastically over-stresses induced in the specimen at the tab tip. In the gage length, stresses vary widely, this result explains on its own the broad discrepancies that has been observed in the GARTEUR program [1].

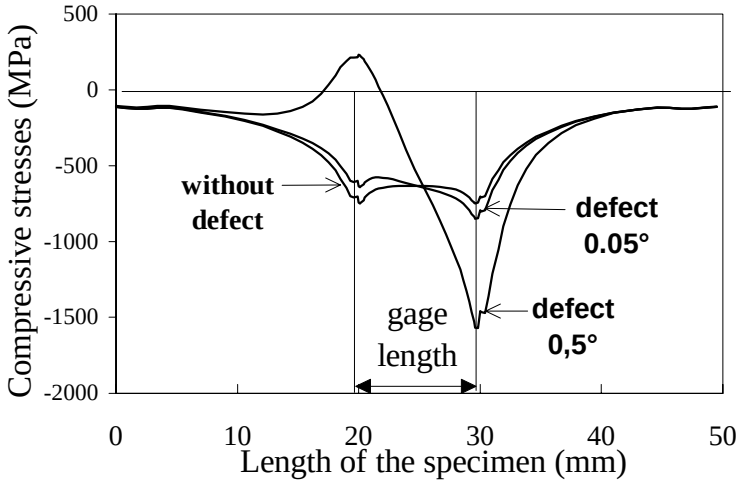


*Fig. 2: Influence of positioning defect of compression plates on specimen stress distribution.*

A series of computations on various geometries demonstrates the major role played by the adhesive (thickness, stiffness, geometry) on the stress distribution. To get a uniform stress state, maximum in the specimen gage length, the glue layer thickness must be increased (1mm at the least), have a highly tapered aspect (tapering angle lower than 12°) and be soft enough (lower than 3000 Mpa). Following these recommendations we propose a new design of the 'Aérospatiale test fixture' (Fig. 3-b), yielding a uniform loading maximum in the specimen gage length while avoiding buckling. Tabs and grips are tapered and the gage length is slightly reduced from 10 to 8 mm. Over-stressed zones no longer exist and the stress state in the gage length is compressive uniaxial. In the adhesive layer the shear level exceeds the shear strength, but the area of these high shear stresses is much lesser than in the initial test fixture. Development of damage is delayed and thus combined loading is preserved for a longer time. 0.5° defect also induces large over-stresses at the tab tip but to a lesser extent. Experimentally various shapes of grips are tested, but failure unfortunately takes place in the grips. Tridimensionnal measurements [7] showed that positioning defects prevented any good result to be reached. Mainly, the necessary clearance of the grips in the cylinders used for alignment is a source of imperfections. Lot of work is still necessary to improve the accuracy.

To characterise the compressive strength under bending loading, we also developed a pin-ended buckling device. To systematically reach failure on the face under compression it was

chosen to block the hinge rotation (Fig. 4). This clamping increases the compressive part of the loading. A short series of tests has permitted to establish the influence of both stacking sequence and thickness under a bending-compression loading. Measured ultimate strains are in good agreement with those from ONERA and University of Bristol (UK, Wisnom).

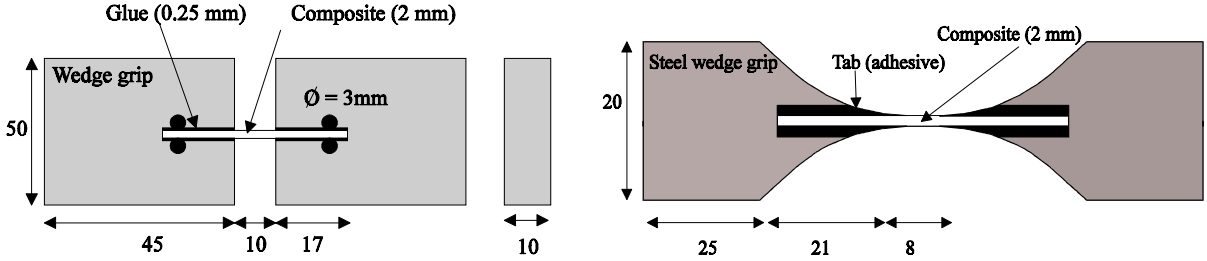


*Fig. 3 : (a) Aérospatiale test fixture and (b) new test fixture configuration.*

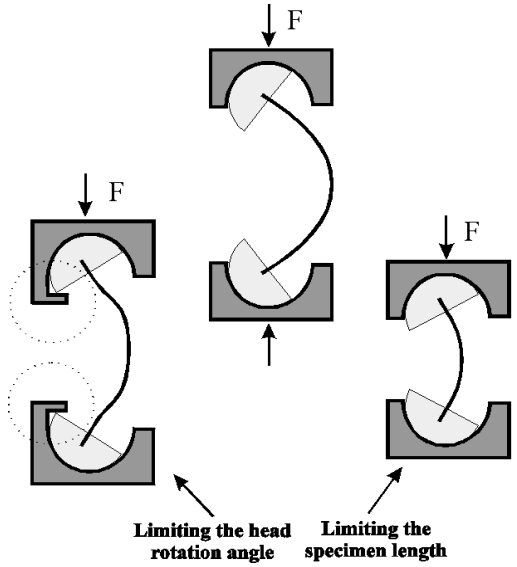


*Fig. 4 : Modifications of the pin-ended buckling fixture.*

## COMPARISON OF PREDICTIONS VERSUS MEASUREMENTS

What follows is concerned with prediction of microbuckling development in laminates. The full thickness is discretised and free-edge conditions are prescribed on both top and bottom faces. Influence of imperfection distribution and structure effect on the instability development is studied separately for simplicity concerns. Initial geometric imperfections are chosen accordingly to measurements from Ref. 16 : wavelength of 0.9 mm and angles from 0.5 to 1.5°. The only unknown parameter is the imperfection distribution across the thickness which has never been measured. Following the understanding of imperfection brought by Ref. 17, a parabolic distribution is chosen with a maximum amplitude at mid-thickness. Then the influence of the loading, the thickness and the stacking sequence on the compressive strength of laminates is presented. Realistic constitutive laws are used for quantitative comparisons of our predictions with measurements from our test [7] and from Ref. 4.

### Loading

Experiments show that locally laminates of T300/914 type can withstand more than 2% of compressive strain under bending loading, and about 1.2% when loaded with pure

compression fixtures. This effect is demonstrated on a 3.2 mm thick UD modelled first for a constant loading across the thickness (pure compression) and second for a linear variation (pure bending). In Fig. 5, which shows failure strains from various simulations, it is clear that for the two loadings the larger the imperfection, the lower the compressive strength. But main the result is that for any imperfection the compressive strength under flexural loading is larger than for compression loading. With an imperfection angle close to 0.5° the predicted strength agrees very well with experimental measurements : 1.95% for bending and 1.2% for compression. Predictions of kink-band models (here Ref. 18) are close to values commonly obtained with pure compression test fixtures (Fig. 4).

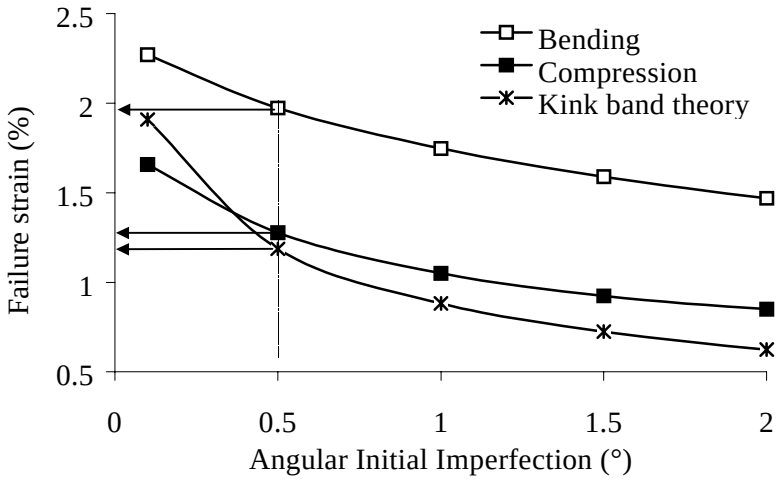


*Fig. 5 : Failure strain versus imperfection angle for compression and pure bending loadings.*

Difference in strength for the two types of loading is almost constant whatever the imperfection angle considered. This is due to stress and strain distributions across the thickness that are characteristic of each loading and independent of the imperfection. Under pure compressive loading, strain and stress distributions are fixed by the imperfection distribution through the thickness. Matrix plasticity revealing the development of microbuckling spreads all over the laminate thickness but does not localise in the boundary layers as could be expected from elastic modes [11]. Conversely under bending loading the plastic flow area is reduced to a third of the total thickness, in the most compressed zone : the gradient of loading sets the transverse characteristic length upon which microbuckling develops. This agrees with Ref. 11 where elastic microbuckling modes are studied and with Ref. 12 where the same conclusions are reached for imperfect UDs. This influence of the loading gradient on the compressive strength put to the fore by Ref. 5 has recently been confirmed experimentally by Ref. 6 and Ref. 7 who used a specific test fixture.

Influence of the imperfection angles on the compressive strength under bending and compression loadings are similar. This important result suggests that the high scatter of compressive strength measurements observed with various pure compression devices [1] can be attributed to test fixtures and not only to fibre imperfections.

**Thickness**

To evaluate the effect of ply thickness on the characteristic transverse length computations are carried out on UD with thickness varying from 0.25 to 12.8 mm. Three imperfection angles are considered (0.5°, 1° and 1.5°). Predictions are compared with bending tests results from Ref. 4 and Ref. 7 respectively carried out on XAS/913 and T300/914 UDs. Mean fibre

characteristics between XAS and T300 are used to compute the strength reported in Fig. 6 .

Under pure compression loading, thickness has very little influence on the compressive strength (Fig. 5). Constant stress and strain distributions across the thickness are observed as stated previously. Except for the influence of the boundary layers for thin UD (≤ 1 mm), there is no structure effect under pure compression, for no characteristic transverse length is induced. Only the imperfection distribution across the thickness can induce a structural effect.

Conversely, under bending loading decreasing laminate thickness induces an increase of the failure strain for 0.5° imperfection as well as for 1.5°. This higher strength is caused by the smaller zone loaded in compression when thickness is decreased, in other words when the gradient of loading increases. Over 3.2mm the influence of the thickness becomes smaller.

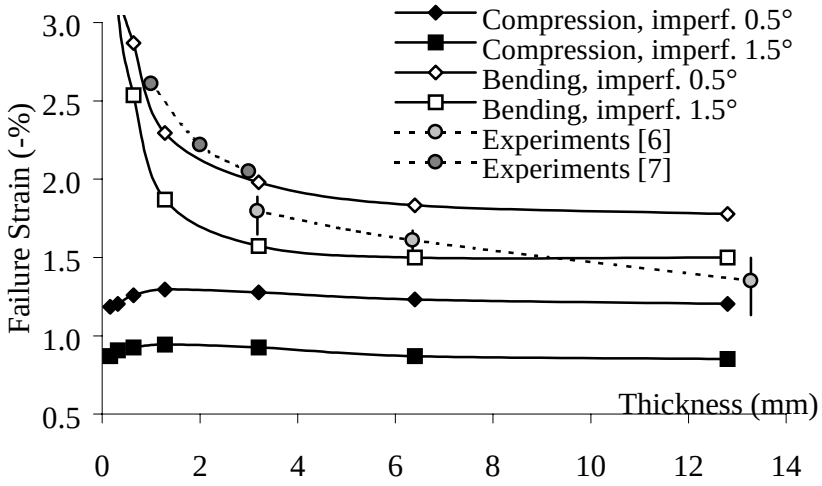


*Fig. 6. Failure strain versus UD thickness.*

In Fig. 6 it clearly appears that our predictions correlate well with experimental measurements from both Ref. 6 and Ref. 7, regardless of the small drop between experimental measurements due to slight difference in constituent characteristics. When thickness is the largest (over 12mm), the low experimental strength is related either to manufacturing flaws or to the presence of large amplitude imperfections as suggested by our predictions and as it was observed on thick composites.

**Stacking sequence**

Here, we investigate the influence of both the stacking sequence and the transverse plies stiffness (90° and 45°). Five laminates made up of 16 T300/914 plies are considered : $[0_{16}]$, $[0_2,45_2]_{2S}$, $[0_2,90_2]_{2S}$, $[0,90_3]_{2S}$, $[0,90]_{4S}$. Among these laminates, three families can be distinguished which are characterised by the number of 0° consecutive plies: 16, 2 and 1 ply. Experiments are carried out with our pin-ended buckling fixture where failure systematically occurs on compressed face. Strain gradients of loading measured at failure are fairly constant.

Whatever the loading, the thicker the 0° consecutive plies the lower the laminate strength (Fig. 7). Presence of 90° or 45° cross plies sets the characteristic transverse length by clamping transverse displacements in the vicinity of the interface with 0° plies. Orientation of these cross plies have a similar negligible influence on the instability since $[0_2,45_2]_{2S}$ and $[0_2,90_2]_{2S}$ strength are very close. In contrast the transverse plies thickness have a strong influence on the mechanism.

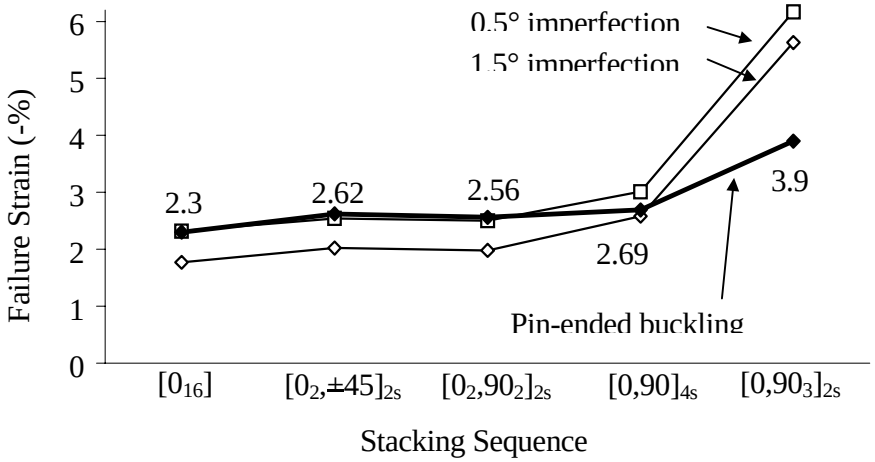


*Fig. 7. Failure strain both predicted (for 2 imperfections) and measured for a bending-compression loading, versus a decreasing number of consecutive 0° plies (16, 2, 1).*

## CONCLUSION

Final results from both theoretical and experimental works have been presented. A modelling approach of the compressive failure has been built which allows for quantitative predictions with very little computational effort. Results for laminates provide a reliable explanation of the high strength obtained under bending loading. Applied loading coupled with the laminate thickness and the stacking sequence results in fixing the dimension of the zone where plastic microbuckling develops and therefore sets the whole strength. Whatever the loading considered the effect of the imperfection on the compressive strength is of the same order; this confirms that wide scatters observed for experimental measurements are mainly caused by the testing devices themselves as it has been demonstrated in this work.

For cross-plies laminates the number of consecutive plies in the loading direction is the key parameter. More precisely, the total thickness of these consecutive plies sets the characteristic transverse length over which microbuckling can develop and which influence this development under compressive or flexural loading. Experimental measurements obtained with our in-house modified pin-ended buckling very well agree with theoretical predictions. The mechanism of failure in laminates under compression or bending is perfectly described provided more information can be obtained on the geometrical imperfection. Last developments on this subject are described in a paper of the present book [17].

## REFERENCES

1. ‘t Hart W.J.G., Aoki R., Bookholt H. , Curtis P.T., Krober I., Marks N., and Sigety P. "Garteur compression behaviour of advanced CRFP", AGARD Report 785. The utilisation of advanced composites in military aircraft. *73rd Meeting of the AGARD Structures and Materials Panel held in San Diego,* 7th-11th October 1991.

2. Effendi R. R. , "Analyse des mécanismes de dégradation en compression des composites unidirectionnels fibres de carbone-matrice organique et modélisation associée", *Thèse de Doctorat de l'Ecole Nationale Supérieure de l'Aéronautique et de l'Espace,* 1993.

3. Grandsire-Vinçon I., "Compression des composites unidirectionnels : méthodes

d'essais et approche micromécanique", *Thèse de Doctorat de l'ENS Cachan*, 1993.

4. Wisnom M.R., "The effect of the specimen size on the bending strength of unidirectional carbon fibre-epoxy",. *Comp. Struct.*, Vol. 18, pp 47-63, 1991.

5. Grandidier J.-C., " Compression et microflambage dans les matériaux composites à fibres longues" , *Thèse de l'Université de Metz*, 1991.

6. Wisnom M.R., "Reduction in compressive strain to failure of unidirectional carbon fibre-epoxy with increasing specimen size in pin-ended buckling tests", *Comp. Sci. Techn.*, Vol. 57 (9/10), pp 1303-1308, 1997.

7. Anthoine-Rahier O., "Amélioration des montages d'essais de caractérisation de la résistance en compression des composites stratifiés. Mise en évidence de l'effet de structure", *Thèse de l'Université Louis Pasteur de Strasbourg*, 5 Janvier 1998.

8. Argon A. S., "Fracture of composites", *Treatise of Materials Science and Technology*, Vol. 1, Academic Press, New-York., 1972

9. Budiansky B., "Micromechanics", *Computers and Structures*, vol. 16, pp 3-12, 1983.

10. Grandidier J.-C., Potier-Ferry M., and Ferron G., "Microbuckling and strength in long-fiber-composites : theory and experiments", *Int. J. Solids Struct.*, Vol. 29 (14/15), pp 1753-1761, 1992

11. Drapier S., Grandidier J.-C., Gardin C., Potier-Ferry M., "Microbuckling and structure effect", *Comp. Sci. Techn*, Vol. 56, pp 861-867, 1996

12. Drapier S., Grandidier J.-C., Potier-Ferry M., " Towards a numerical model of the compressive strength for long-fibre composites ", *Eur. J. Mech/A*, Vol. 18 (1), pp 1159-1164, 1999.

13. Kyriakides S., Arseculeratne R., Perry E.J., and Liechti K.M., "On the compressive failure of fiber reinforced composites", *Int. J. Solids Struct.*, Vol. 32 (6/7), pp 689-738, 1995.

14. Gardin C., Potier-Ferry M., "Microflambage des fibres dans un matériau composite à fibres longues : analyse asymptotique 2-D", *C. Rend. Acad. Sc. Paris*, t.315, Série II, pp 1159-1164, 1992.

15. Hutchinson J.W., "Plastic buckling", *Advances in Applied Mechanics*. Vol. 14, pp 67-144, 1974.

16. Paluch B., "Analyse des imperfections géométriques affectant les fibres dans un matériau composite à renfort unidirectionel", *La Recherche Aéronautique*, Vol 6, pp 431-448, 1994.

17. Jochum C. Grandidier J.-C. and Potier-Ferry M., "Modelling approach of microbuckling mechanism during cure in carbon/epoxy laminates", *ICCM12 July 5$^{th}$-9$^{th}$*,1999.

18. Budiansky B., and Fleck N.A., "Compressive Failure of Fiber Composites", *J. Mech. Phys. Solids*, Vol. 41, pp 183-211, 1993.